ISSN: 0974-5823 Vol. 7 No. 7 July, 2022)

International Journal of Mechanical Engineering

Study The Effect of Multi Axial Cycling Loading on The Dynamic Crack Propagation In Aluminum Plates

Rafid Ibrahim Mhawes

University of Baghdad/College of Engineering, Mechanical Engineering Department

Dr. Fathi A. Alshamma

University of Baghdad/College of Engineering, Mechanical Engineering Department

Abstract

Fatigue is the foremost failure cause in structural mechanics, in this paper the dynamic crack growth due to multi-axial cyclic loading for thin plates was studied. The material of plates used are aluminum alloys and the fracture mechanics of the cracks propagated are considered, the operating life of materials is studied via the a-N curve. The experimental work was performed using a new suggested test rig, which was designed to apply the cyclic shear load (zero-based and repeated) and constant tension. Furthermore, the stress intensity factor, K_c, for modes I and II, the Paris Law parameters (i.e. c and m), and the da/dN crack growth per cycle were found experimentally. These are used in analyzing the problem using ABAQUS software. The speed of crack propagation, at the secondary stage of the crack life, is found analytically, numerically, and experimentally. The validity of the results is approved by comparing the numerical with the experimental one.

1. Introduction

Aluminum alloys are widely used in space structures [1, 2]. To study the crack propagation in the structural elements, it is necessary to have good knowledge about the stress distribution near the crack tip and how fast the crack propagated under the applied loads under time or cycles. Typically experiments show that the crack growth rate is constant during time excluding the last unstable stage [3]. Cracks (or microscopic defects) may be due to physical defects during the production process, so it is unavoidable and should be taken into account [4]. This may cause structural failure as they grow over time. Detecting these defects in the member doesn't mean that no longer use this part safely anymore. Therefore, crack propagation learning enables us to know how long the cracks may reach a critical value. In this work, a test rig that can apply multiaxial cyclic load was designed and used to satisfy these requirements. The manufacturing of this rig is mainly based on two design factors, the first one is functionality, while the latter is the specimen configuration [5, 6]. Pre-existent central cracks were studied in a plate that was subjected to different loading, i.e. uniaxial or multiaxial, in the proposed specimens the crack grow non-uniformly, at both sides, per cycles (da/dN) and/or direction [7-9]. This is due to mixed-mode conditions [8]. In this work, a central crack under multiaxial cyclic loading for aluminum alloys was studied theoretically, numerically, and experimentally.

2. Theoretical Analysis

In this section, the theoretical analysis for studying the dynamic crack growth under multi-axial cyclic loading is considered. A crack of length 5 mm and width 1mm was created by a wire-cut machine and located 35 mm from the end of the shear load grippers, as shown in Fig. 1. Considering Griffith energy criterion with an infinitely large brittle material plate that contains a single sharp through-crack is assumed [10], Fig. (1).

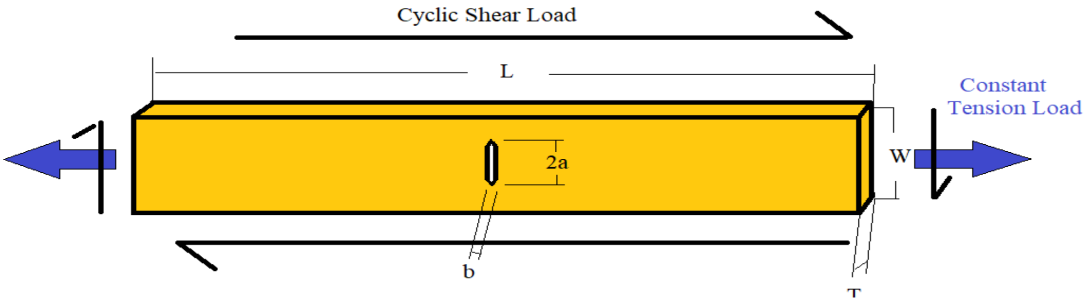

Figure (1) the theoretical solution for non-proportional multiaxial loading

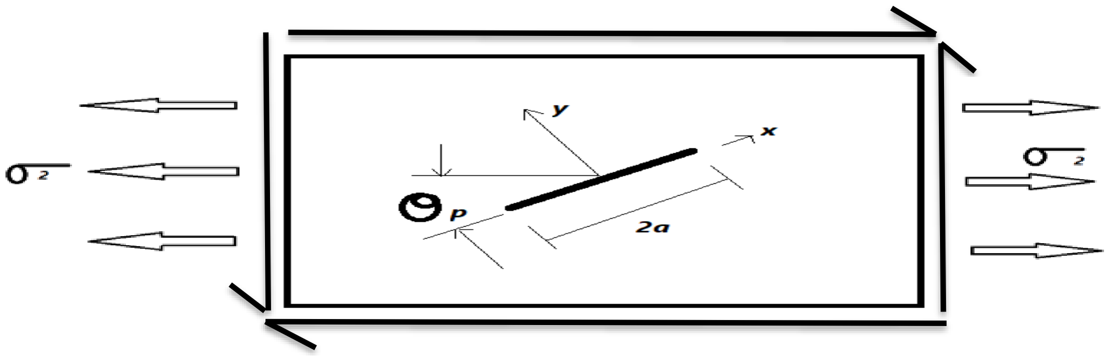

Figure (2) The multi-axial cycling loading principle stresses are expressed as [11]:

$K_I = \sigma_n\sqrt{\pi a}$-- (1)

$K_{II}=\tau\sqrt{\pi a}$--- (2)

$\sigma_n = \sigma cos^2 \propto$-- (3)

$\tau = \tau_{x\,\sin\propto\,\cos\propto}$-- (4)

$\sigma_{1,2} = \frac{\sigma_x+\sigma_y}{2} \pm \sqrt{(\frac{\sigma_x-\sigma_y}{2})^2 + \tau_{xy}{}^2}$ ------------------------------------ (5)

These stresses correspond to a plane expressed as:

$\tan 2\theta_p = \frac{2\tau_{xy}}{\sigma_x-\sigma_y}$ --- (6)

The principal stresses for the present study are:

$\sigma_{1,2} = \frac{\sigma}{2} \pm \sqrt{(\frac{\sigma}{2})^2 + (\tau_{xy}\sin(\frac{\omega t}{2}))^2}$ ------------------------------- (7)

These stresses correspond to a plane expressed as:

$\tan 2\theta_p = \frac{2(\tau_{xy}\sin(\omega t/2))}{\sigma}$ --- (8)

According to equation (3) the angle of inclination of the principal plane is varied depending on ωt. As the crack orientation in the plate along the y-axis, therefore the crack orientation coincides with the plane of principal stresses, i.e. angle θ_p, as shown in Figure (4).

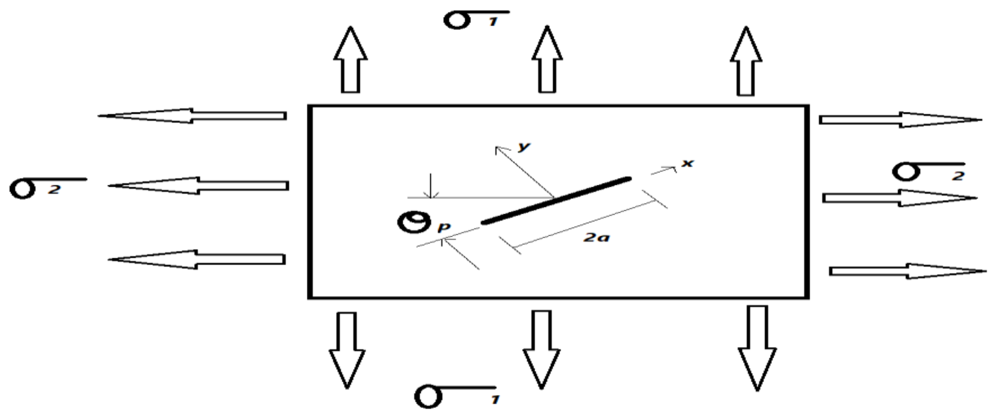

Figure (3)Plate subjected to biaxial stresses with inclined crack

If $\sigma_2 = \alpha\sigma_1$, (σ_2 is compressive stress), therefore, for modes I and mode II, the stress intensity factor are represented by the following:

$K_I = \frac{\sigma_1\sqrt{\pi a}}{2}\{(1+\alpha)+(1-\alpha)\cos 2\theta_p\}$ ----------------------------------- (9)

$K_{II} = \frac{\sigma_1\sqrt{\pi a}}{2}\{(1-\alpha)\sin 2\theta_p\}$ --- (10)

$\Delta K_I = K_I max - K_I min$ --- (11)

$\Delta K_{II} = K_{II} max - K_{II} min$ --- (12)

The maximum values of $K_I max$ and $K_{II} max$ are found at $\sin\omega t = 1$, while the minimum values correspond to $\sin\omega t$ As a result, [11]:

$\Delta K_{eq} = \sqrt{\Delta K_I{}^2 + \Delta K_{II}{}^2}$ -- (13)

Using Paris law; the crack growth can be expressed as:

$\frac{\partial a}{\partial N} = C\,(\Delta K_{eq})^m$ -- (14)

$\frac{\partial a}{\partial N}$ was measured experimentally, and *C* and *m* are obtained for the present loading by plotting log $\frac{\partial a}{\partial N}$ against log ΔK_{eq} , the slope of the line represents *m,* and *C* can be found from the intersect of the line with the log $\frac{\partial a}{\partial N}$. Using equation (3-10), by taking in the consideration the value of (N) number of revolutions per minute.

Table 1: Mechanical properties of Al-7050

E (GPa)	σ_y (MPa)	(σ_u) (MPa)	Poisson's ratio(ν)	Density (ρ) kg/m^3
73.3	325	360	0.33	2.726

Table 2 : Mechanical properties of Al-7075

E (GPa)	σ_y (MPa)	(σ_u) (MPa)	Poisson's ratio(ν)	Density (ρ) kg/m^3
81.5	486	560	0.33	2780

3.Analytical Solutions

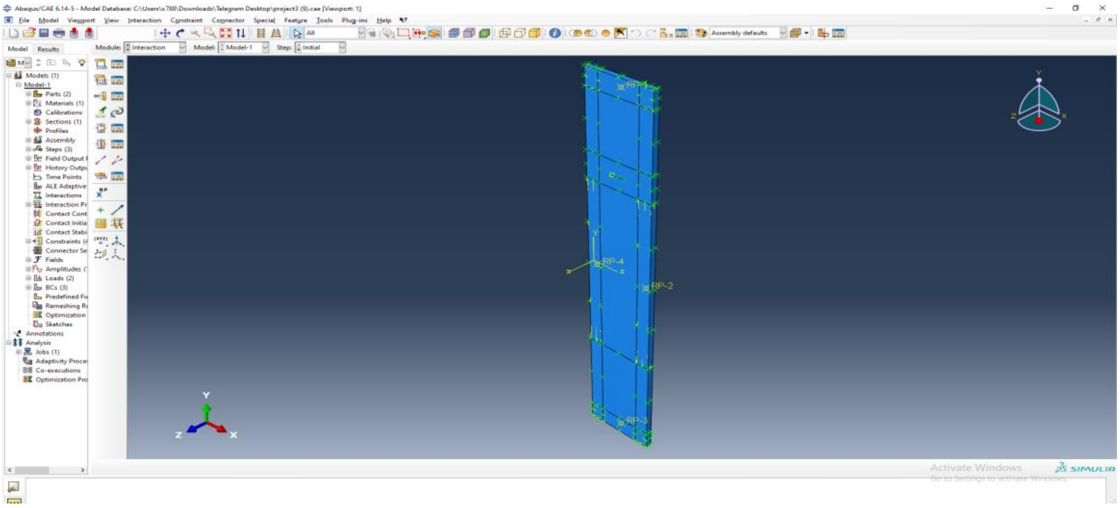

Figure (4)

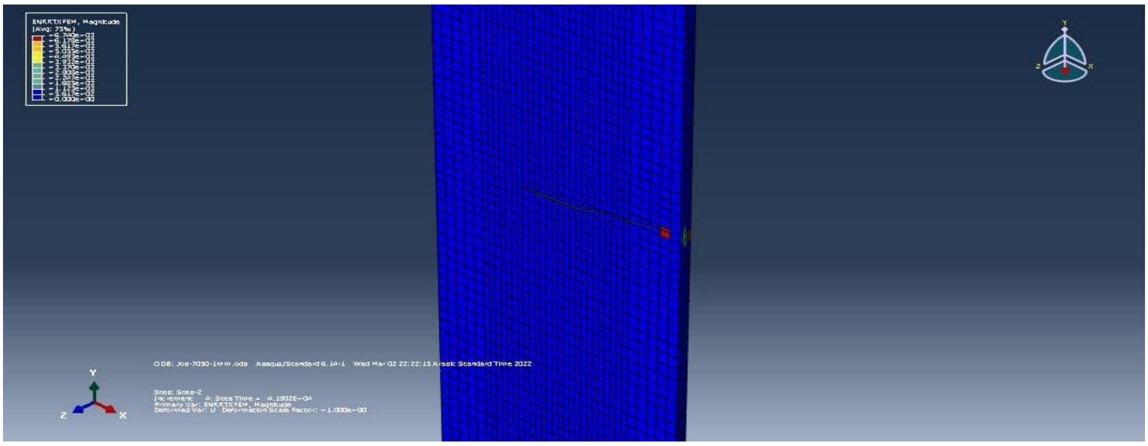

Figure (5)

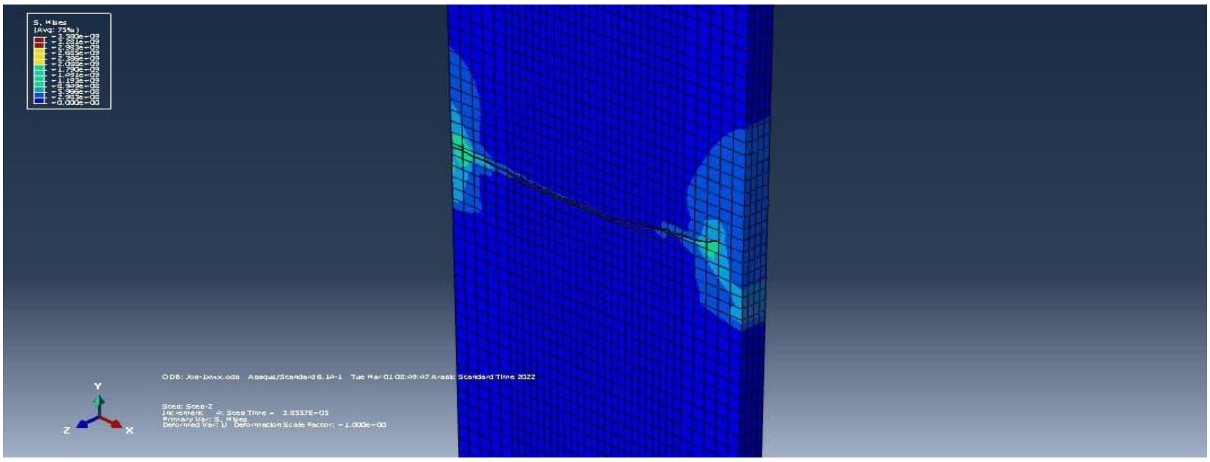

Figure (6)

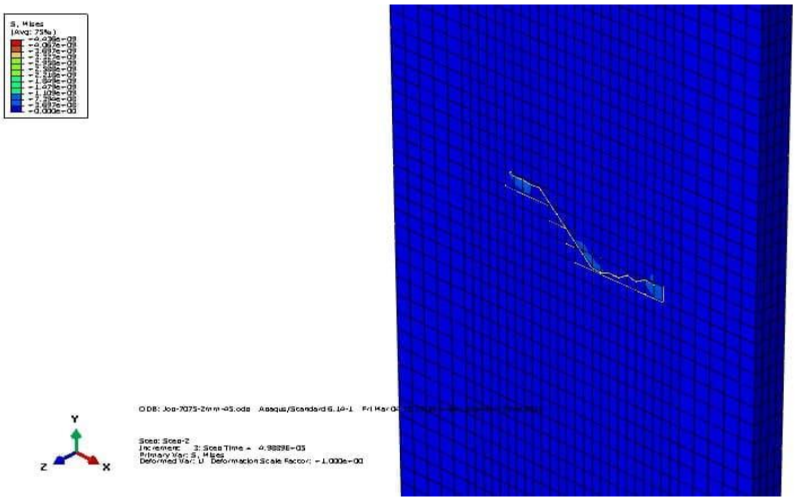

Figure (7)

4. Experimental Work

In the present work, a test rig is specially designed and manufactured for applying multi-axial cyclic loads. Two aluminum alloys were used, 7050 as well as 7075, as testing plates, their dimensions were 150 mm long, 25 mm width, and 2 mm thickness. The chemical composition and tensile tests were performed for these plates. An incision of a length of 5 mm was made in the middle of the plates to study the crack propagation experimentally.

The experimental value of the intensity factor K_{eff} for Modes I and Mode II (crack length 2*a* =5mm) was obtained and used. Paris Law constant (*C* and *m*) were evaluated using a digital Camera (Dino) that used for finding Log (da/dN), Log (K) for these plates were calculated theoretically as shown in Table 2. K_{eff} for mode I was found applying a tensile load at a speed of 0.01mm/sec. Dino Camera was fixed at the test rig to monitor the cracks growing. K_{eff} for mode II was also calculated. New grippers were designed to apply the corresponding shear load. The test rig was designed and manufactured for applying the multiaxial cyclic load this enables to study of the fracture mechanics in the three modes. Mode I (opening the crack) corresponds to in-plane tension loads, Mode II is for shear and Mode III for tier loads. In this study, linear elastic fracture mechanics are considered for Mode I and II (plane stress). A constant tension load of 30 MPa is applied, while the cyclic loading is considered as shear one; the shear load fluctuates from Zero to the maximum value of 80 MPa. These forces are applied via a mechanism that is specially designed for this purpose, the speed of the Three-Phase AC motor (2HP and 3000 r.p.m) is controlled, the motor is connected to the crankshaft via V-belt, the motion is transmitted to slot link to apply the shear force via shear's gripper, a dial gauge is fixed at its end, as shown in Fig. 6. A constant tension load is applied by a manual hydraulic pressing machine via a tension Gripper. Another gripper is secured on the sliding base, as shown in Fig. 6.

Figure (8) Multiaxial load cyclic load mechanism

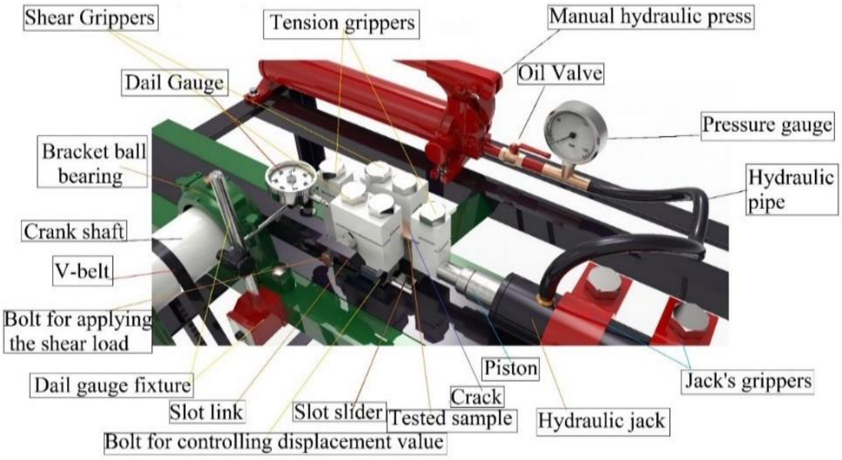

Fig (9) Close view of Grippers

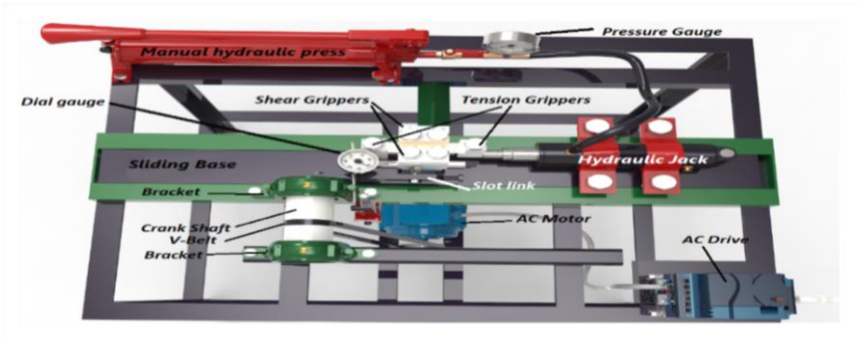

Figure (10) Top view of Multi-axial Cyclic load Machine

The procedure of testing are: firstly apply 30 MPa constant tension, then tightened the grippers of the shear load, after that the motor speed is adjusted to 1000 r.p.m, the speed was measured via a Tachometer, which was used for reading the rotational speed of the crankshaft). A dial gauge was secured at the end of shear grippers, the reading of the dial gauge was performed via a slow-motion video camera that records it during working (0.2 mm repeated). The crack was cutted at one-third of the used samples, the crack dimensions: 0.7 mm width, 5 mm length, and 2 mm depth,

5. **Results:**

In this section of the research ;the results that obtained from capplaing nonproportional cycling loading on the 7050 and 7075 with different thickness of 1 dnd 2 mm which have been solved theoretically using analytical and numerical analysis and then experimentally to verified the results for finding the velocity of crack propagation and the equation of dynamic crack growth by using ΔK_{eq}. From fig(11) Which gives the relation between theoretical. experimental and the numerical results for (a-n) (a-dk);(a_dk) and (da/dn –dk) ; have been shown that have illustrate the behavior of the crack growth to be low number of cycles when compared with the figures (12) While the effect of the principle stress and depend on the value of where (α) the theoretical and numerical results have very closed results when compared with each other. Also in fig(13)Shows the effect of different material properties on the same thickness of 2mm and have significant effect and more pronounced when the crack is 45 dig for move non operational angle (14)
And this is because the brittleness and low toughness for the material on the dynamic crack growth and the direction of extended crack when there is move effect the ration of (σ_n) to the (τ_n) which depend on the stress ratio ($\sigma_/ \tau$) siuwt and on the value of the maximum amplitude of the cycling shear stress so that the value

of the constant for the elecdi on between the (da/dn) with (ΔK_{eq}) will vary and depend on the rate of increase which have obtained from the slope of a with dk and an/dn with dk for fig(15) shown the dependent of the thickness of the specimens on the crack propagation which will increase the ratio of ($\sigma_{/}\ \tau_{sinwt}$) but for the same time the behavior of the crack growth will be move near to the elastic – plastic and then the blanded of the crack tip will change the direction of the crack growth and have more cycles when compared with the same material of thickness 2mm in this study the main object is to find the constants of the relation da/dn with dk and the rate of increase in its values when the crack is inclined with angle 45 which is move effect on the results.

6. **Conclusion**

Dynamic crack propagation is importance for designing members that subjected to cyclic loading. Application of cycling load occurs in automobiles cylinder, aircraft wings, bridges, and machines structures. Prediction of such a complex behavior especially when the parts are subjected to multi-axial cyclic loading is a task that requires extensive experimental and theoretical work. Experimental investigations of the present work were performed on aluminum alloys plate series 7050 and 7075 with a central crack. The plates are subjected to a cycling shear load combined with constant tensile stress, the stress coefficient depends on the crack rate that is affected by the stress at the crack tip. The cyclic loading has a great effect on the crack growth, especially when the part or members are subjected to multi-axial cyclic loading. To study this problem a test rig was designed and manufactured to apply cyclic shear load accompanied with constant tension. This device enables the monitoring of the crack growth and calculating the critical stress intensity factor ΔKc for modes I and II.

Theoretical works included modifying the dynamic crack growth equation of that modified to account for multi-axial cyclic loading to predict the a-N curve. Alternatively, numerical analysis, via ABAQUS software, enables the simulation of the crack model and finding crack growth using the Paris Law parameters (c, m, ΔK, and da/dN).

7. Disclosure

The ABAQUS Program and MATLAB software were used in this study.

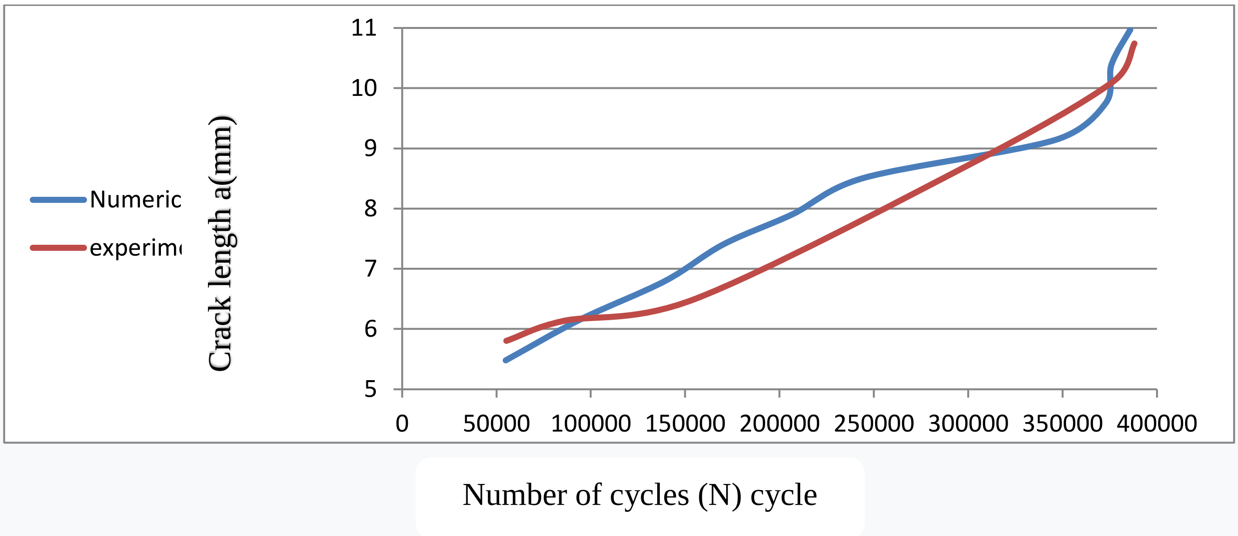

Figure (11) Crack Length .No. Of Cycles Al 7050 t (2mm) (a-n)

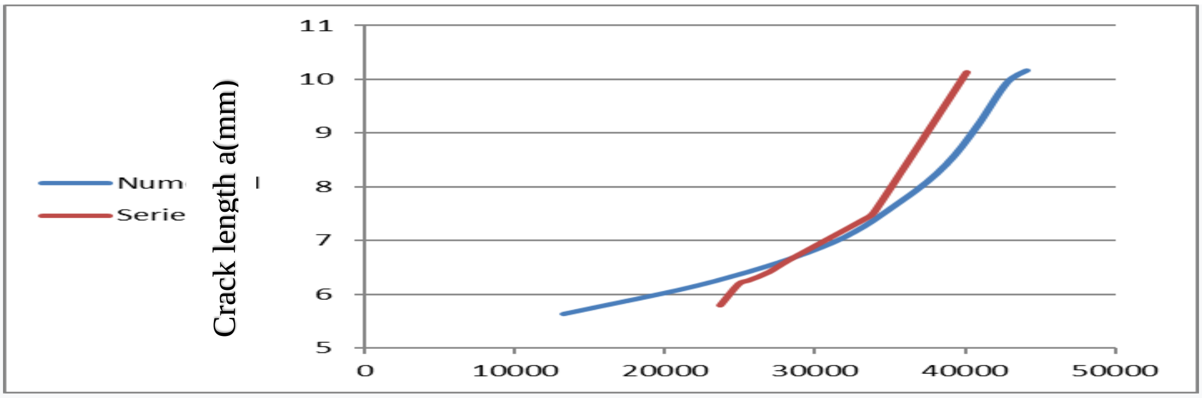

Number of cycles (N) cycle

Figure (12) Crack Length .No. Of Cycles Al 7050 t (2mm) (45 deg) (a-n)

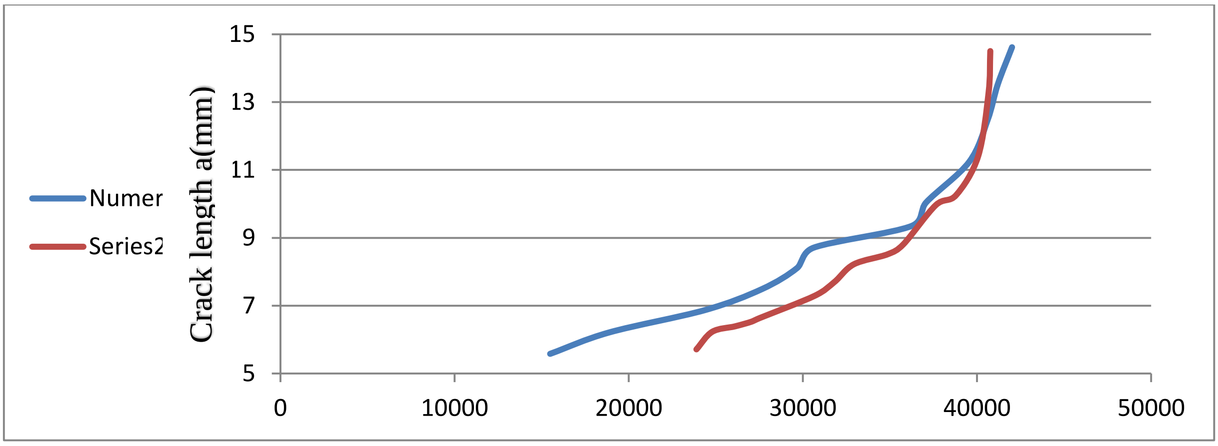

Number of cycles (N) cycle

Figure (13) Crack Length . No. Of Cycles Al 7050 t (1mm) (a-n)

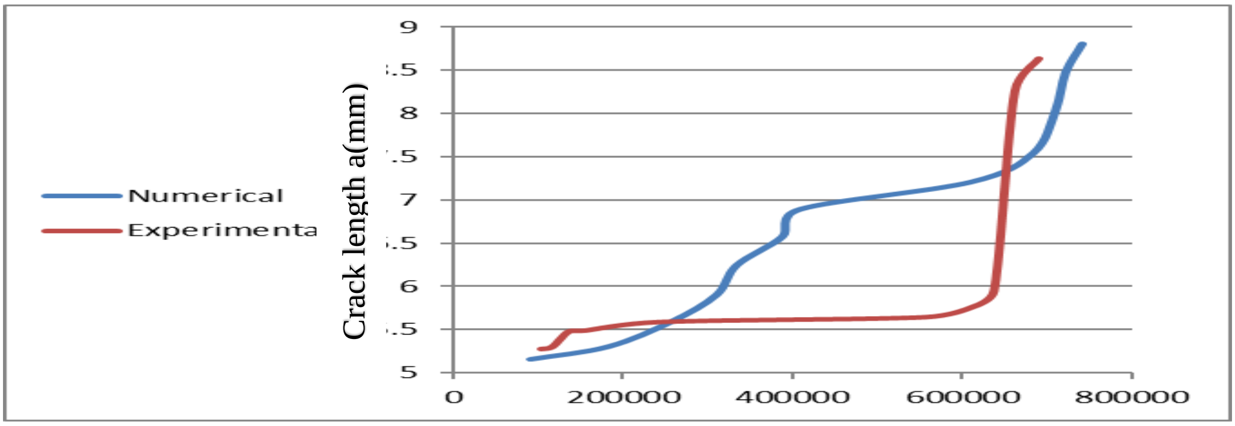

Number of cycles (N) cycle

Figure (14) Crack Length . No. Of CyclesAl 7075 t (2mm) (a-n)

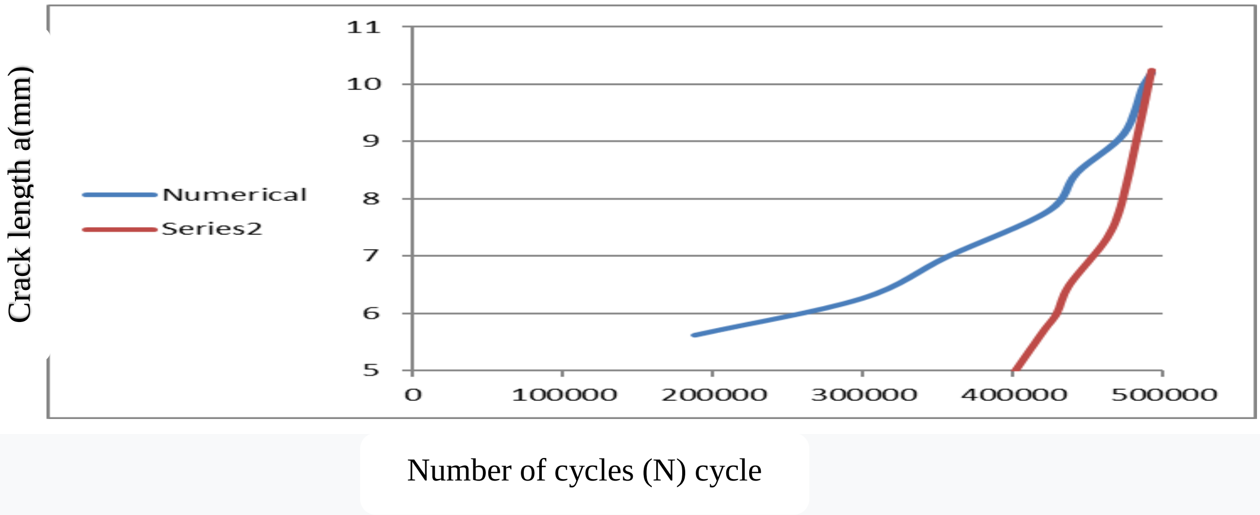

Figure (15) Crack Length . No. Of CyclesAl 7075 t (2mm) (45 deg) (a-n)

References

[1] Sunil Kumar Singhal, Maneet Lal, Indu Sharma and Rakesh Behari Mathur "***Fabrication of copper matrix composites reinforced with carbon nanotubes using a combination of molecular-level-mixing and high energy ball milling"*** Journal of Composite Materials, DOI: 10.1177/0021998312443397, May2012.

[2] Susumu Arai and Takuma Osaki ***"Fabrication of Copper/Multiwalled Carbon Nanotube Composites Containing Different Sized Nanotubes by Electroless Deposition",*** Journal of the Electrochemical Society, 162 (1) D68-D73, Nov.2015.

[3] Liangfu Zheng, Jianren Sun, Quanfang Chen ***"Carbon nanotubes reinforced copper composite with uniform CNT distribution and high yield of fabrication"***, Micro & Nano Letters · DOI: 10.1049/mnl.2017.0317, May 2017.

[4] Ali Samer Muhsan, Faiz Ahmad, NoraniM.Mohamed, Puteri Sri Melor Megat Yusoff, and Muhammad Rafi Raza ***"Uniform Dispersion of Multiwalled Carbon Nanotubes in Copper Matrix Nanocomposites Using Metal Injection Molding Technique",*** Hindawi Publishing Corporation, International Journal of Manufacturing Engineering,Volume 2013, Article ID 386141,9 pages , Aug 2013.

[5] Pyry-Mikko Hannula , Antti Peltonen , Jari Aromaa , Dawid Janas , Mari Lundstrom , Benjamin P. Wilson , Krzysztof Koziol , Olof Forsen ***"Carbon nanotube-copper composites by electrodeposition on carbon nanotube fibers"*** ,Carbon-Elsevier, Carbon 107 (2016) 281e287,June-2016.

[6] Meet Lal • S. K. Singhal • Indu Sharma • R. B. Mathur ***"An alternative improved method for the homogeneous dispersion of CNTs in Cu matrix for the fabrication of Cu/CNTs composites"***. Springer, March 2012.

[7] Kai Liu, Yinghui Sun, Ruifeng Zhou, Hanyu Zhu, JiapingWang, Liang Liu, Shoushan Fan1and Kaili Jiang "**Carbon nanotube yarns with high tensile strength made by a twisting and shrinking"** Nanotechnology 21 (2010) 045708(7pp), doi:10.1088/09574484/21 /4/045708, Des 2009.

[8] Ragab A. and Bayoumi S., ***''Engineering Solid Mechanics''***, CRC Press, 1998.

[9] Rozumek D. , Marciniak Z., and Macha E., ***''Fatigue Crack Growth Rate In Non-Proportional Bending With Torsion Loading''***, 17th European Conference, Czech Republic, 2008.

[10] De Pauw J., De Baets P. and De Waele W., ***''Review and Classification of Fretting Fatigue Test Rigs''***, Sustainable Construction and Design, 2.1:41, 2011.

[11] Blazic M., Maksimovic S., Petrovic Z., Vasovic I., and Turnic D., ***''Determination of Fatigue Crack Growth Trajectory and Residual Life under Mixed Modes''***, Journal of Mechanical Engineering, DOI:10.5545/sv-jme.2013.1354, Vol. 60, pp. 250-254, 2014.

[12] Bruhm EF. Analysis and design of flight vehicle structures Indianapolis: Jacobs publishing Inc:1973